International Journal of Automotive Technology, Vol. 8, No. 6, pp. 761–769 (2007)

1229-9138/2007/037-11

PERFORMANCE CHARACTERISTICS OF A PROTON EXCHANGE MEMBRANE FUEL CELL (PEMFC) WITH AN INTERDIGITATED FLOW CHANNEL

P. H. LEE, S. A. CHO, S. S. HAN and S. S. HWANG*

Department of Mechanical Engineering, University of Incheon, Incheon 402-749, Korea

(Received 12 June 2007; Revised 21 October 2007)

ABSTRACT–The configuration of the flow channel on a bipolar plate of a proton exchange membrane fuel cell (PEMFC) for efficient reactant supply has great influence on the performance of the fuel cell. Recent demand for higher energy density fuel cells requires an increase in current density at mid voltage range and a decrease in concentration overvoltage at high current density. Therefore, an interdigitated flow channel where mass transfer rate by convection through a gas diffusion layer is greater than the mass transfer by a diffusion mechanism through a gas diffusion layer was recently proposed. This study attempts to analyze the i-V performance, mass transfer and pressure drop in interdigitated flow channels by developing a fully three dimensional simulation model for PEMFC that can deal with anode and cathode flow together. The results indicate that the trade off between performance and pressure loss should be considered for efficient design of flow channels. Although the performance of the fuel cell with interdigitated flow is better than that with conventional flow channels due to a strong mass transfer rate by convection across a gas diffusion layer, there is also an increase in friction due to the strong convection through the porous diffusion layer accompanied by a larger pressure drop along the flow channel. It was evident that the proper selection of the ratio of channel and rib width under counter flow conditions in the fuel cell with interdigitated flow are necessary to optimize the interdigitated flow field design.

KEY WORDS: PEMFC, Interdigitated flow channel, Pressure drop, Counter-flow

NOMENCLATURE

a_K : activity of water
A_{CV} : specific face area of the control volume (c.v.), m^{-1}
C_{wK} : concentration of water at K membrane interface, mol/m^3
D_w : diffusion coefficient of water, m^2/s
F : Faraday constant, 96,487 C/gm-equivalent
I : local current density, A/m^2
I_0 : exchange current density for the oxygen reaction, A/m^2
J : diffusion mass flux, kg/m^2-s
m : mass fraction of the species
M : molecular weight, kg/kmol
P : total pressure, atm
M_{mdry} : equivalent weight of a dry membrane, kg/ kmole
P_{O2} : partial pressure of oxygen, atm
R : gas constant, 8.314 J/mol/K
$P^{sat}_{w,K}$: vapor pressure of water in k channel, atm
t_m : membrane thickness, m
T : temperature
n_d : electro-osmotic drag coefficient (number of water molecules carried per proton)
η : overpotential for oxygen reaction, V
σ_m : membrane conductivity, 1/ohm/m

*Corresponding author. e-mail: hwang@incheon.ac.kr

1. INTRODUCTION

The PEMFC (Proton Exchange Membrane Fuel Cell) using a very thin polymer membrane is considered to be a promising candidate for transportation applications and residential power in future power plants. This type of fuel cell has many advantages such as high efficiency, low temperature operation, and it is clean, quiet, and capable of quick startup. However, performance and durability under harsh environments and high cost should be optimized in order to be competitive with conventional combustion power sources.

A typical schematic of a PEMFC is shown in Figure 1. The cell is a sandwich of two graphite bipolar plates with small flow channels separated by a MEA (Membrane Electrode Assembly) which consists of a membrane and two electrodes with a dispersed Pt catalyst. The gas diffusion layer (GDL) is porous to supply reactants to the electrodes at unexposed areas of the flow channel.

It is well known that flow channel design including

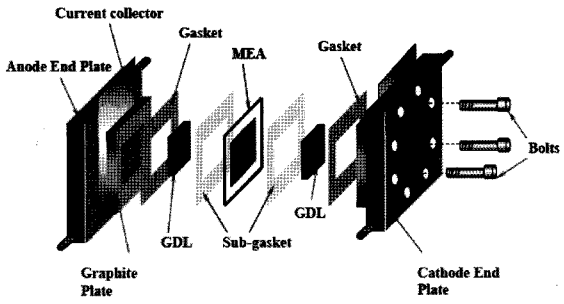

Figure 1. Schematic of a fuel cell assembly displaying different essential components of the system.

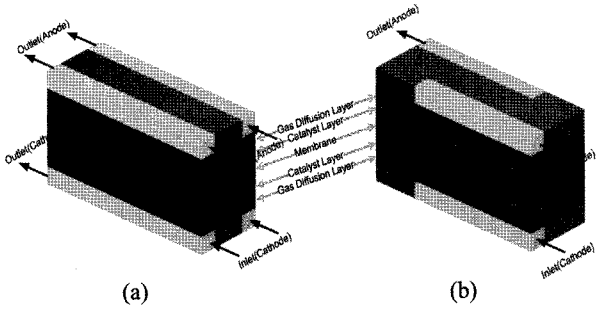

(a) (b)

Figure 2. Schematic of the flow channel structure: (a) Parallel flow channel; (b) Interdigitated flow channel.

GDL is very important to supply reactants and expel products effectively, and hence directly affects the performance of the fuel cell.

Therefore, many investigations have been done to determine the optimal flow channel configuration. Most studies on flow channels have been focused on parallel and serpentine flow channels (Springer *et al.*, 1991; Fuller and Newman, 1993; Nguyen and White, 1993; Yi and Nguyen, 1998). Recent demand on higher energy density fuel cell requires the increase in current density at mid voltage range and a decrease in concentration over voltage at high current density.

Therefore, an interdigitated flow channel where mass transfer rate by convection inside a gas diffusion layer is greater than that by a diffusion mechanism through a gas diffusion layer was recently proposed.

Figure 2 shows the comparison of parallel and interdigitated flow structure. Although the main mass transport of reactants in the parallel flow channel takes place by a diffusion mechanism, reactants in the interdigitated flow channel are known to be transported to electrodes by the convective flow through GDL between adjacent channels.

Experimental results (Trung and Nguyen, 1996) for the interdigitated flow channel show that the fuel cell with an interdigitated channel has better performance for its advantages in mass transport. Based on Nguyen's experiment, some numerical studies have been conducted to determine the flow and mass transport mechanism.

(Kazim *et al.*, 1999; Yi and Nguyen, 1999) have developed a two dimensional numerical model to calculate the flow field in an interdigitated channel. This two dimensional approach could not consider the three dimensional flow pattern through GDL, thus its application is limited. (Um and Wang, 2000) have focused on developing a three dimensional numerical model for PEMFC with conventional and interdigitated channels. They revealed that the benefit of this design is enhanced water removal from the flooded catalyst layer and increased usage of active area located under the current collecting rib. (Hu and Fan, 2004) found that the convection transport mechanism is dominant for interdigitated field design, but the diffusion transport is dominant for the conventional flow field design.

The above studies of interdigitated flow channel design have focused on mass transfer and the density distribution of hydrogen and oxygen only at the cathode. It is thought that the interaction between anode and cathode flow is of crucial importance to simulate realistic performance characteristics. This study attempts to analyze the i-V performance, mass transfer and pressure drop in interdigitated flow channels by developing a fully three dimensional simulation model for PEMFC that can deal with anode and cathode flow together.

A commercial program, FLUENT (Version 6.2), was modified using user-defined functions in order to simulate three dimensional characteristics of PEMFC with the parallel flow channel and the interdigitated flow channel (Um, 2003; Lee and Dutta *et al.*, 1999; Shimpalee *et al.*, 1999, 2000; Lee and Vanzee, 1999; Dutta *et al.*, 2001; Kim *et al.*, 2006). For optimal interdigitated flow field design, the effects of the flow direction at both the anode and the cathode, such as co-flow and counter flow, are considered and the ratio of the channel width and rib was adjusted in order to determine its effects on performance. In addition, the effects of the operating temperature and humidity on the performance were examined as well.

2. NUMERICAL MODELS

Governing equations for calculating the fully three dimensional flow field are expressed under the following assumptions.

(1) The gas mixture is incompressible, ideal fluid
(2) The flow in the flow channel is laminar
(3) Isothermal conditions exist
(4) Butler-Volmer kinetics predominate for the electrochemical reaction rate.

2.1. Mass Conservation Equation

$$\nabla \cdot (\varepsilon \rho u) = S_m \tag{1}$$

Where ε is the porosity of porous materials. S_m denotes source terms corresponding to the consumption of hydrogen and oxygen in the anode and cathode, and the production of water in the cathode.

$$S_m=S_{H_2}+S_{aw}: Anode \tag{2}$$

$$S_m=S_{O_2}+S_{aw}: Cathode \tag{3}$$

2.2. Momentum Conservation Equation

The fluid flow in the fuel cell is described using the following equation based on Darcy's law (Rawool and Pharoah, 2006).

$$\nabla(\varepsilon\rho\vec{u}\vec{u})=-\varepsilon\nabla p+\nabla(\varepsilon\rho\nabla\vec{u})+S_u \tag{4}$$

Where S_u is expressed as

$$S_{ux}=-\frac{\mu u}{\beta_x},\ S_{uy}=-\frac{\mu v}{\beta_y},\ S_{uz}=-\frac{\mu w}{\beta_z} \tag{5}$$

2.3. Species Conservation Equation

$$\nabla(\varepsilon\vec{u}C_k)=\nabla(D_k^{eff}\nabla C_k)+S_k \tag{6}$$

Where source term S_k denotes,

$$S_k=\begin{cases} -\frac{I(x,y)}{2F}M_{H_2}A_{cv}:S_{H_2} \\ -\frac{\alpha(x,y)}{F}I(x,y)M_{H_2O}A_{cv}:S_{aW} \\ -\frac{I(x,y)}{4F}M_{O_2}A_{cv}:S_{O_2} \\ \frac{1+2\alpha(x,y)}{2F}I(x,y)M_{H_2O}A_{cv}:S_{cW} \end{cases} \tag{7}$$

Current density $I(x,y)$ is described as

$$I(x,y)=\frac{\sigma}{t_m}\{E-V_c-\eta(x,y)\} \tag{8}$$

Where $\alpha(x,y)$ is expressed as

$$\alpha(x,y)=n_d-\frac{F}{I(x,y)}D_w(x,y)\frac{C_{w_c}-C_{w_a}}{t_m} \tag{9}$$

Expressions for water transport and other variables are listed in Table 1.

2.4. Numerical Analysis

Figure 3 shows the computational mesh for the parallel and interdigitated flow channels, respectively. The orthogonal non-uniform grids for computational domain are employed. The dimensions of the flow channel are set to 0.0762 (cm) × 0.0762 (cm) × 4 (cm). The flow channels of the anode and cathode are divided into 40 × 50 × 24.

At the inlets, the fluid is supposed to flow into the channel at a known velocity and the atmospheric pressure is applied at the outlets. Other specifications necessary for calculation are shown in Table 2.

3. DISCUSSIONS

For a validation check of the numerical simulation model used in this study, the performance curves were compared with the experimental data of the fuel cell with the serpentine flow channel obtained under the same conditions as shown in Figure 4. The computed polarization

Table 1. Equation for modeling electrochemical effects.

Water activity	$\alpha=\frac{P_{H_2O}}{P}$	(10)
Nernst quation	$E=E_0+\frac{RT}{2F}\times\ln\left(\frac{P_{H_2}\times P_{O_2}^{1/2}}{P_{H_2O}}\right)$	(11)
Water content in the membrane	$C_w=\left(\frac{\rho_{m,dry}}{M_{m,dry}}\right)\times\lambda$	(12)
Electro-osmotic drag coefficient	$n_d=0.00029\times\lambda^2+0.05\times\lambda-3.4\times10^{-19}$	(13)
Water content in the membrane	$\lambda=0.043+17.81a_a-39.85a_a^2+36.0a_a^3$ $0<a_a<1=14.0+1.4(a_a-1.0)\ :\ 1<a_a\leq3$	(14)
Membrane conductivity	$\sigma=\left(0.00514\times\frac{M_{m,dry}}{\rho_{m,dry}}\times C_w-0.00326\right)\times\exp\left(1268\left(\frac{1}{303}-\frac{1}{T_s}\right)\right)\times100$	(15)
Over potential	$\eta(x,y)=\frac{RT}{F}\ln\left[\frac{I(x,y)P(x,y)}{I_0P_{O_2}(x,y)}\right]: Anode\ Side$ $=\frac{RT}{0.5F}\ln\left[\frac{I(x,y)P(x,y)}{I_0P_{O_2}(x,y)}\right]: Cathode\ Side$	(16)
Back diffusion	$\frac{F}{I(x,y)}\times D_w\times\frac{(C_{w0}-C_{w1})}{t_m}$	(17)

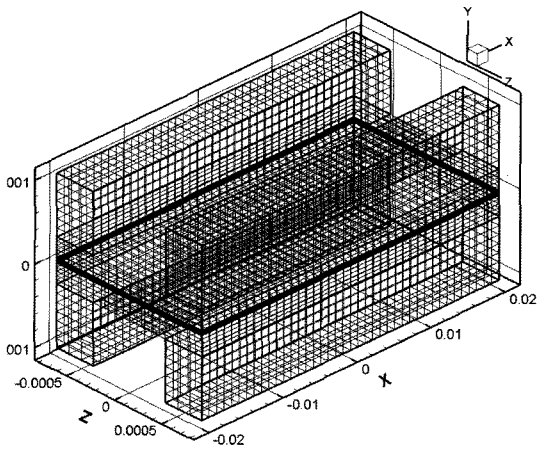

(a)

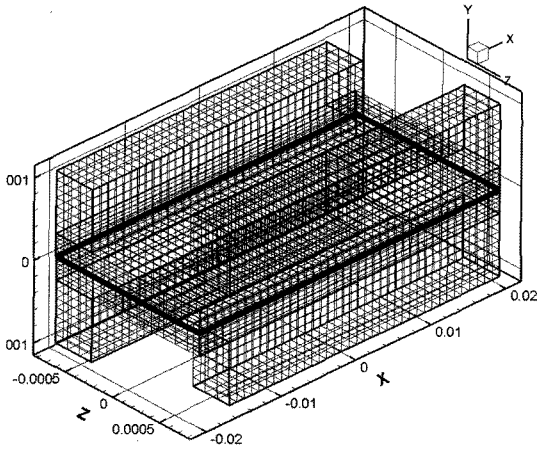

(b)

Figure 3. Computational grids for parallel (a) and interdigitated flow channel (b).

Table 2. Physical parameters.

Description	Value
Channel length (cm)	4
Channel width (cm)	0.0762
Channel height (cm)	0.0762
GDL thickness (cm)	0.0254
Catalyst layer thickness (cm)	0.00287
Inlet temperature (K)	353.15
Anode side pressure (atm)	1
Cathode side pressure (atm)	1
Anode stoichiometric flow rate	1.5
Cathode stoichiometric flow rate	2
O_2/N_2 ratio	0.21/0.79
H_2 inlet mass fraction, Anode (%)	11.54
H_2O inlet mass fraction, Anode (%)	88.46
O_2 inlet mass fraction, Cathode (%)	23.3

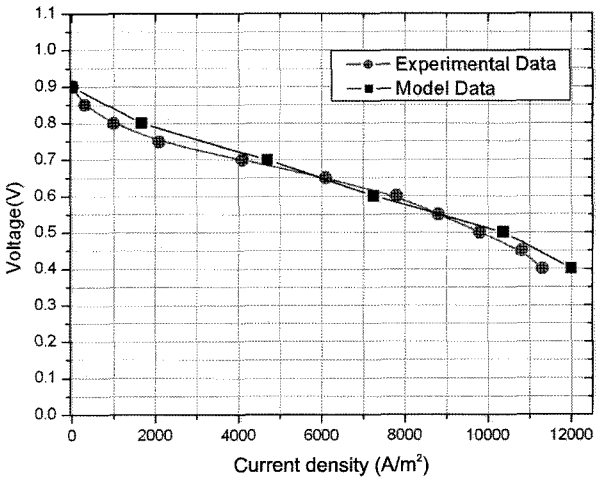

Figure 4. Comparison of experimental and simulated polarization curves.

curve agrees favorably with the experimental polarization curve (Wang *et al.*, 2003). However, at high current density, the difference between the modeling results and experimental data increases, and the model always over-predicts the current density. At a high current density region, the low current density of the experimental results may be caused by the presence of liquid water in the catalyst layers and the gas diffusion layers. Due to the presence of liquid water, the effective porosity of the gas diffusion layers and catalyst layers reduces and the mass transfer resistance increases. Since the current model neglects the above two phase effect, predicted current density at high current density will always be higher than experimental current density (Ticianelli *et al.*, 1988; Wang *et al.*, 2003).

However, comparison of the relative performance of the fuel cell with different flow configurations using a single phase model may give data necessary for the design of the flow channel.

Using this numerical simulation model and the inlet conditions listed in Table 2, numerical simulations were carried out for examining parallel and interdigitated flow fields.

The performance of the two types of flow channels under co-flow conditions was simulated numerically. Average current density for an interdigitated flow channel at 0.5 V is shown to be higher than for a parallel flow channel. To compare the mass transport inside the MEA of the two flow channels, the velocity distribution at the central section along the flow direction of each flow channel was presented (Figure 5). The velocity vector in the parallel flow channel in Figure 5(a) is going toward the membrane and has a symmetric shape, which indicates that most reactants are transported by a diffusion process.

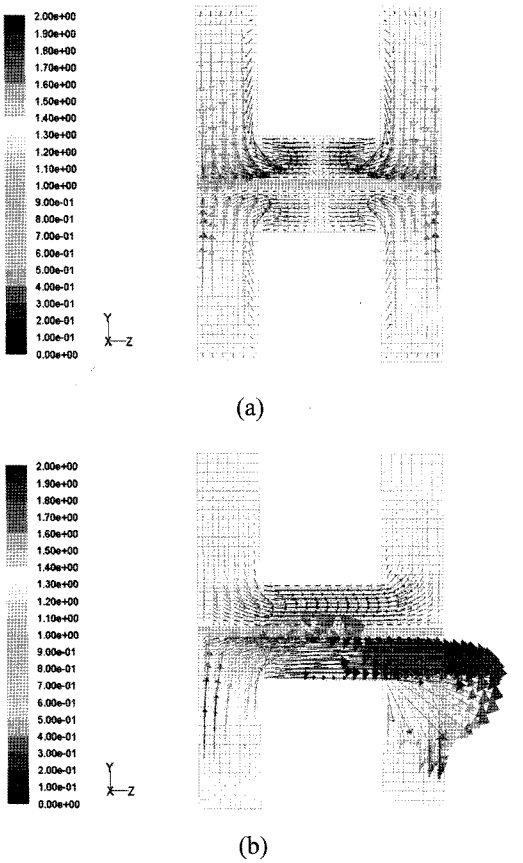

Figure 5. Two-dimensional velocity field in the flow channel at z=L/2: (a) Parallel flow channel; (b) Interdigitated flow channel.

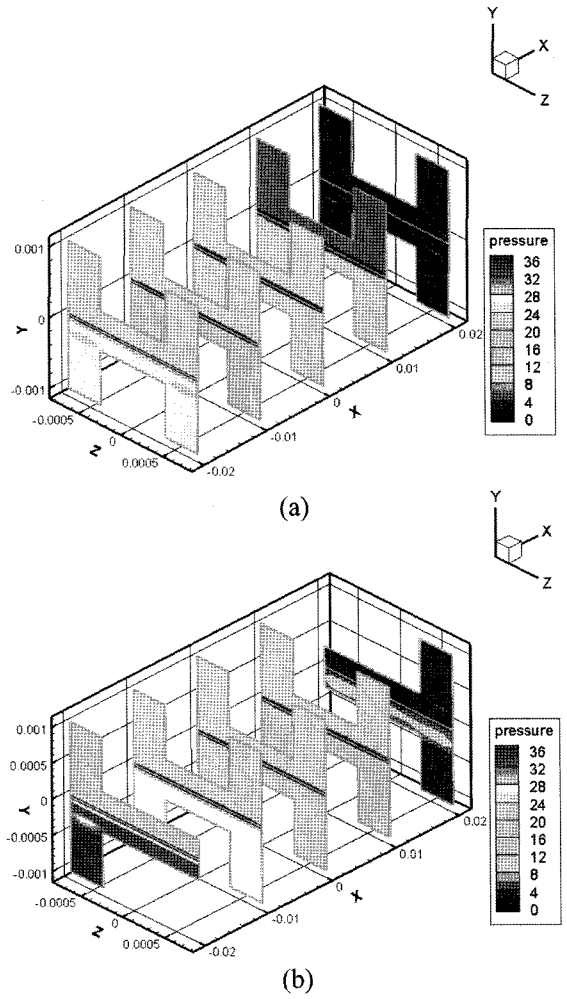

Figure 6. Three dimensional distribution of pressure drop for parallel(a) and interdigitated flow channel.

On the other hand, for the interdigitated flow field in Figure 5(b), strong velocity vectors across the GDL moving toward the adjacent channel are observed. This strong flow is channeled inside the GDL and is thought to be caused by convective transport, which has a higher mass transfer rate. This convective transport makes the mass transport of hydrogen and oxygen into the catalyst layer more effective.

It is important to know the pressure loss in each channel since a higher pressure loss requires a higher pumping power. In order to compare the pressure loss caused by diffusion and convection flow in parallel and interdigitated flow channels, the pressure drop at each channel is presented in Figure 6. Pressure drop in the parallel flow channel is 11Pa at the anode and 23 Pa at the cathode, while the pressure drop in an interdigitated flow channel is 22 Pa at the anode and 36 Pa at the cathode. This higher pressure drop for interdigitated flow is believed to be caused by strong convective flow across the GDL as shown in Figure 5.

While a higher fuel supply by interdigitated flow improves performance due to the higher mass transfer by convection flow, it also accompanies a higher pressure drop in the channel.

In order to compare performance over the entire range of voltage of the parallel flow channel and interdigitated flow channel, polarization curves of each channel under co-flow conditions were presented in Figure 7. The current densities between a parallel and an interdigitated cathode are almost the same until the cell voltage of 0.6 V, because the cell polarization for current densities below 7,000 A/m^2 is dominated by cathode kinetic overvoltage and ohmic polarization. Concentration loss at high current density, >7,000 A/m^2, is known to be caused by the limitation of mass transfer supplied to the cathode electrode. It is thought that enhanced mass transfer caused by the strong convective flow in interdigitaed flow channel tends to reduce concentration loss (Um and Wang, 2004; Hu and Fan, 2004). In this region, the current density of the interdigitated flow channel was higher than that of the

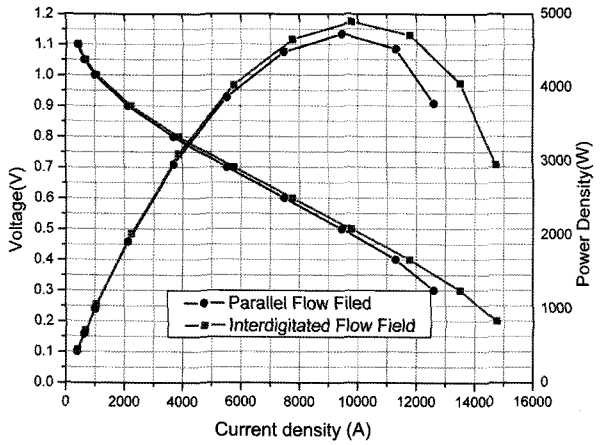

Figure 7. Polarization and power density curves for Parallel flow channel and Interdigitated flow channel.

parallel flow channel.

Curent density in parallel and interdigitated flow channels at 0.3 V represent 12,612 A/m^2 and 13,512 A/m^2, respectively.

These results indicate that the trade off between performance and pressure loss should be considered for the efficient design of the flow channel.

Generally, the flow direction at both electrodes is known to be very important for the efficient mass transfer in fuel cells. Consequently, the effect of flow direction was investigated for the performance optimization of interdigitated flow channels. Figure 8 shows the current density distribution on the membrane at 0.5 V under co-flow and counter-flow conditions. In the figure, the current density ranges from 8,000 A/m^2 to 14,000 A/m^2 in the co-flow and from 8,000 A/m^2 to 12,000 A/m^2 in the counter-flow. It is observed that the uniform and higher average current density under counter flow conditions are distributed across the catalyst surface layer because of more efficient mass transfer between the anode and cathode flow channels. Here, the average current density means the total current density divided by the reaction area and it also indicates the overall performance of the fuel cell. The average current density was 9,455 A/m^2 in co-flow and 9,590 A/m^2 in counter-flow.

In order to determine how the flow direction affects electrochemical reactivity, we examined the distribution of molar water concentration at the central section of GDL, which is indicative of reaction activity. Figure 9 shows the density distribution at the central section of

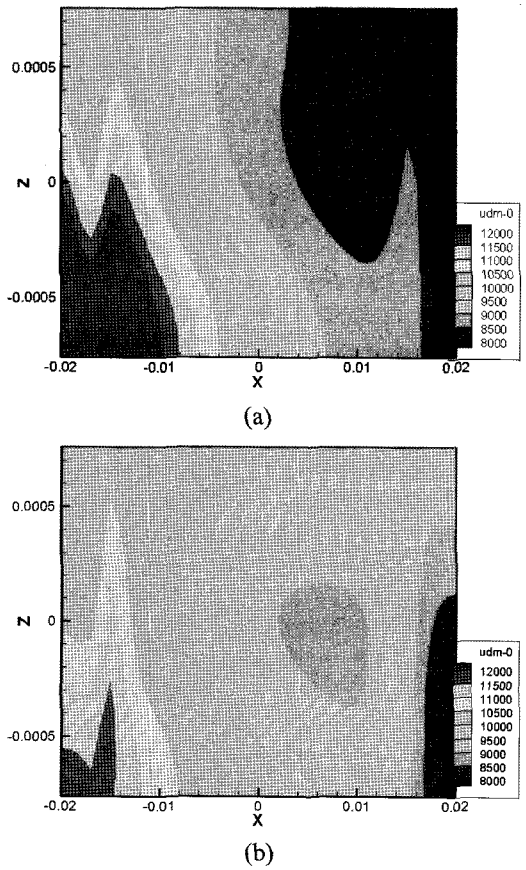

Figure 8. Current density on the MEA at 0.5 V under co-flow (a) and counter flow condition (b).

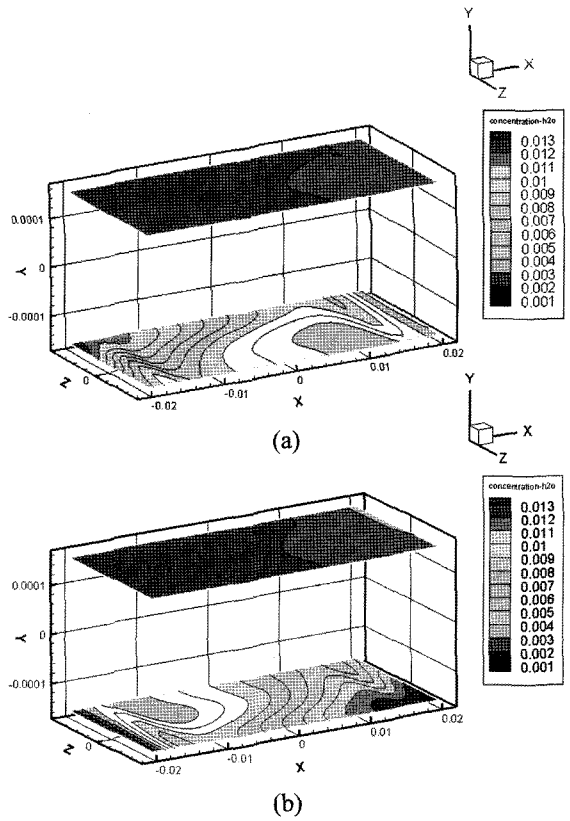

Figure 9. Molar water concentration at GDL at 0.5 V for co-flow (a) and counter flow condition (b).

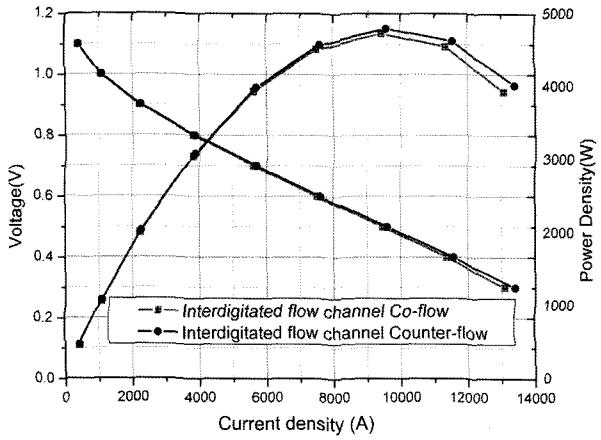

Figure 10. Comparison of performance for interdigitated flow field in co-flowing (a) and counter flowing condition (b).

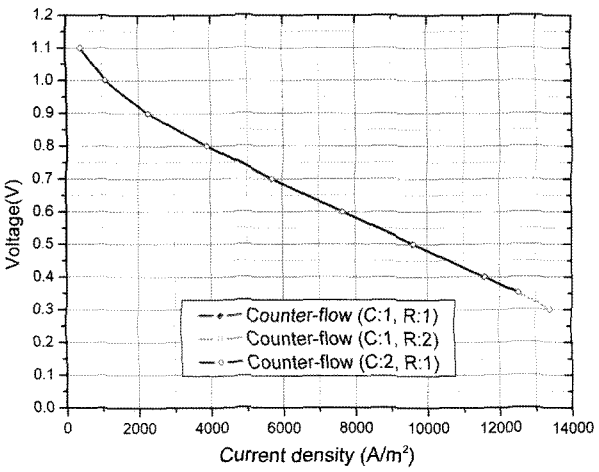

Figure 11. Polarization curves for different ratio of channel and rib width.

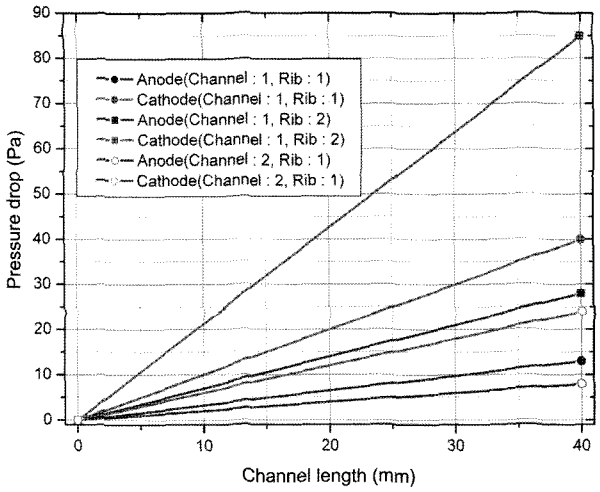

Figure 12. Pressure loss at anode and cathode for different ratio of channel and rib width.

GDL at 0.5 V for co-flow and counter-flow. It shows that at a 100% humidified anode the water density gradually decreases along the longitudinal direction due to the diffusion and convection flow through the membrane. Conversely, at the non-humidified cathode it gradually increases along the flow channel due to water generation by electrochemical reaction.

It is found that the water density at the cathode in counter-flow was generally higher than that in co-flow, which shows that the counter-flow facilitates a more active electrochemical reaction.

Figure 10. shows the i-V curves and the power density of the fuel cell under co-flow and counter-flow conditions. At the high current density region, power density for counter-flow is a little higher than that for co-flow, which coincides to the results of the average current density.

The flow channel shape in the fuel cell is known to have a tremendous effect on pressure loss. Therefore, to elucidate the effect of pressure loss on the shape of the interdigitated flow channel, the ratio of channel width and rib width, which are important variables in the channel shape, were varied for numerical calculations. The ratio of channel and rib was set to 1:1, 1:2, and 2:1. Figure 11 shows the i-V curves according to the ratio of channel to rib. It shows that there is no significant difference in current density within the ratio of the channel width and rib given for this calculation. By contrast, the pressure curve shown in Figure 12 illustrates that as the channel becomes wider relative to the rib width, the pressure drop along the channel is greatly decreased. Pressure loss at the 1:1 ratio is 13Pa at the anode and 40 Pa at the cathode, while the pressure drop at the 1:2 and 2:1 channel/rib ratios are 28 Pa and 8 Pa at the anode, and 85 Pa and 24 Pa at the cathode, respectively.

This means that the effect of the ratio of the channel and the rib should be considered for the reduction of the pressure drop in the interdigitated flow channel. In other words, the conditions for minimizing pressure loss without an appropriate difference in performance should be considered.

Besides the effects of the flow configuration described above, it is very important to identify the effects of operating conditions, such as operating temperature and humidity, for obtaining better performance of fuel cells.

Figure 13 shows a polarization curve according to operating temperature, which is one of the key operating conditions. It is found that the fuel cell performance generally increases as the operating temperature increases. The temperature rise greatly enhances the electrochemical reaction rate leading to an increase in the electron pro-

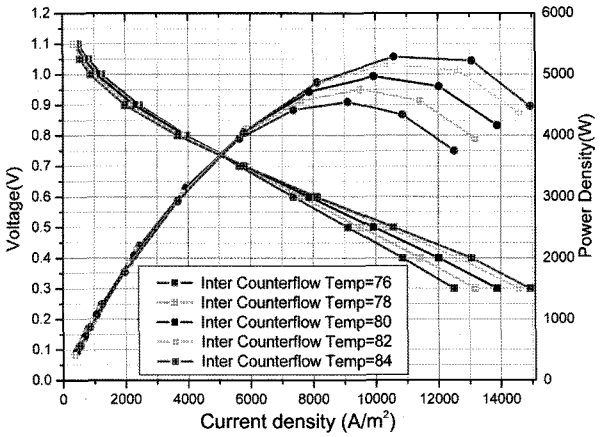

Figure 13. Polarization curves for different temperature.

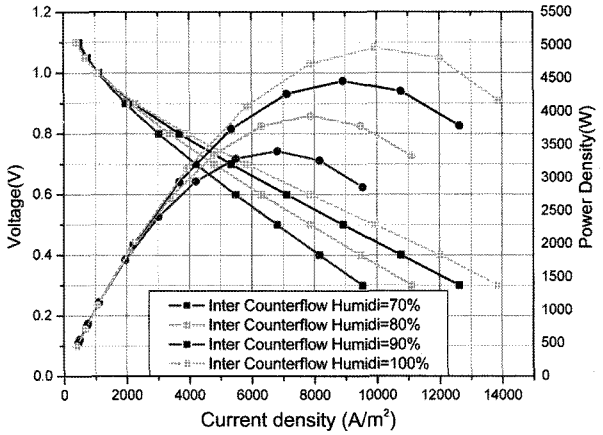

Figure 14. Polarization curves for different humidification.

duction rate. This is because the electrochemical reaction rate increases exponentially with increasing operating temperatures.

A performance analysis by humidity, in Figure 14, shows that performance increases with an increase in humidity. The conductivity of Nafion, which is generally used as a polymer electrolyte of PEMFC, is strongly related to water content and increases linearly along with humidity. This increase in conductivity helps hydrogen ions move more easily and thereby facilitates a higher electron production rate.

4. CONCLUSIONS

By using a single-phase, fully three dimensional simulation model for PEMFC that can deal with anode and cathode flow together, the following conclusions for PEMFC with interdigitated flow channel could be obtained.

(1) A trade off between performance and pressure loss should be considered for efficient design of flow channels. Performance of the fuel cell with interdigitated flow is better than that with a conventional flow channel due to a high mass transfer rate by convection across the gas diffusion layer. However, increase of friction by the strong convection through the porous diffusion layer accompanies a larger pressure drop along the flow channel (Birgersson and Vynnycky, 2006).

(2) It is found that the performance of polymer membrane fuel cells with an interdigitated flow channel is higher in counter-flow than in co-flow conditions. Uniform and higher current density under counter flow conditions is observed to be distributed across the catalyst surface layer because of more efficient mass transfer between the anode and cathode flow channel.

(3) Numerical simulations for the effects of channel and rib width show that pressure drop decreases greatly with increasing channel width of the interdigitated flow channel and the proper design of the ratio of channel and rib width is very important to reduce parasite loss.

(4) Operating temperature and humidity in fuel cells are found to strongly enhance the electrochemical reaction rate and ion conductivity leading to higher electron production rate.

(5) Since our model considers only a single phase, it has some limitations to representing water flooding phenomena properly. However, comparison of the relative performance of a fuel cell with different flow configurations may give the data necessary for the design of a flow channel.

REFERENCES

Birgersson, E. and Vynnycky, M. (2006). A quantitative study of the effect of flow-distributor geometry in the cathode of a PEM fuel cell. *J. Power Soc.*, **153**, 76–88.

Dutta, S., Shimpalee, S. and Van Zee, J. W. (2001). Numerical prediction of mass-exchange between anode and cathode channels in a PEM fuel cell. *Int. J. Heat and Mass Transfer*, **44**, 2029–2042.

Fuller, T. F. and Newman, J. (1993). Water and thermal management in solid polymer electrolyte fuel cells. *J. Electrochem. Soc.*, **140**, 1218–1225.

Hu, G. and Fan, J. (2004). Three-dimensional numerical analysis of proton exchange membrane fuel cell (PEMFCs) with conventional and intrdigitated flow fields. *J. Power Soc.*, **136**, 1–9.

Kazim, A., Liu, H. T. and Forges, P. (1999). Modeling of performance of PEM fuel cells with conventional flow field. *J. Appl. Electrochem.*, **26**, 1409–1416.

Kim, H. G., Kim, Y. S., and Shu, Z. (2006). Simulation of unit cell performance in the polymer electrolyte

membrane fuel cell. *Int. J. Automotive Technology* **7**, **7**, 867–872.

Lee, W. K., Ho, C. H., Zee, J. W. V. and Murthy, M. (1999). The effects of compreddion and gas diffusion layers on the performance of a PEM fuel cell. *J. Power Soc.*, **84**, 45–51.

Lee, W. K., Van Zee, J. W., Shimpalee, S. and Dutta, S. (1999). Effect of humidity on PEM fuel cell performance part I-Experiments. *Int. Mechanical Engineering Congress & Exposition*, 359–366.

Nguyen, T. V. and White, R. E. (1993). A water and heat management models for proton exchange membrane fuel cells. *J. Electrochem. Soc.*, **140**, 2178–2186.

Rawool, A. S., Mitra, S. K. and Pharoah, J. G. (2006). An investigation of convective transport in micro proton-exchange membrane fuel cells. *J. Power Soc.*, **162**, 985.

Srinivasan, S., Ticianelli, E. A., Derouin, C. R. and Redondo, A. (1988). Advances in solid polymer electrolyte fuel cell technology with low platinum loading electrodes. *J. Power Soc.*, **22**, 359–375.

Um, S. (2003). *Computational modeling of Transport and Electrochemical Reaction in Proton Exchange Membrane Fuel Cell.* Ph. D. Dissertation. Penn State University. USA.

Um, S. and Wang, C. Y. (2000). Three dimensional analysis of transport and reaction in proton exchange membrane fuel cells. *Proc. ASME Fuel Cell Division.*

Shimpalee, S., Dutta, S. and Van Zee, J. W. (2000). Numerical prediction of local temperature and current density in a PEM fuel cell. *IMECE, Session of Transport Phenomena in Fuel Cell System*, 26–32.

Shimpalee, S., Dutta, S., Lee, W. K. and Van Zee, J. W. (1999). Effect of humidity on PEM fuel cell performance part I-Numerical simulation. *Proc. ASME IMECH, TN*, HTD 364-1, 367–374.

Springer, T. E., Zawodzinski, T. A. and Gottesfeld, S. (1991). Polymer electrolyte fuel cell model. *J. Electrochem. Soc.*, **138**, 2334–2342.

Trung and Nguyen, V. (1996). A gas distributor design for Proton exchange membrane fuel cell. *J. Electrochem. Soc.*, **143**, L103–L105.

Um, S. and Wang, C. (2004). Three-dimensional analysis of transport and electrochemical reactions in polymer electrolyte fuel cells. *J. Power Soc.*, **125**, 40–51.

Wang, L., Husar, A., Zhou, T. and Liu, H. (2003). A parametric study of PEM fuel cell performances. *Int. J. Hydrogen Energy*, **28**, 1263–1272.

Yi, J. S. and Nguyen, T. V. (1998). An along the channel model for proton exchange membrane fuel cells. *J. Electrochem. Soc.*, **145**, 1149–1159.

Yi, J. S. and Nguyen, T. V. (1999). Multicomponent transport in porous electrodes of proton exchange membrane fuel cell using the interdigitated gas distributors. *J. Electrochem. Soc.*, **146**, 1149–1159.